Electronic Supplementary Material (ESI) for Molecular Systems Design & Engineering.

Supplementary Information

Anchoring and packing of self-assembled monolayers of *semithio*-bambusurils on Au(111)

Pramod Patil Kunturu,[a] Özlem Kap,[b] Kai Sotthewes,[b] Pierre Cazade,[c] Harold J. W. Zandvliet,*[b] Damien Thompson,*[c] Ofer Reany,*[d] and Jurriaan Huskens*[a]

[a] Molecular Nanofabrication Group, MESA + Institute for Nanotechnology, Faculty of Science and Technology, University of Twente, P.O. Box 217, 7500 AE Enschede, The Netherlands.

[b] Physics of Interfaces and Nanomaterials, MESA+ Institute for Nanotechnology, University of Twente, P. O. Box 217, 7500AE Enschede, The Netherlands.

[c] Department of Physics, Bernal Institute, University of Limerick, Limerick V94 T9PX, Ireland.

[d] Department of Natural Sciences, The Open University of Israel, 1 University Road, Ra'anana 43107, Israel.

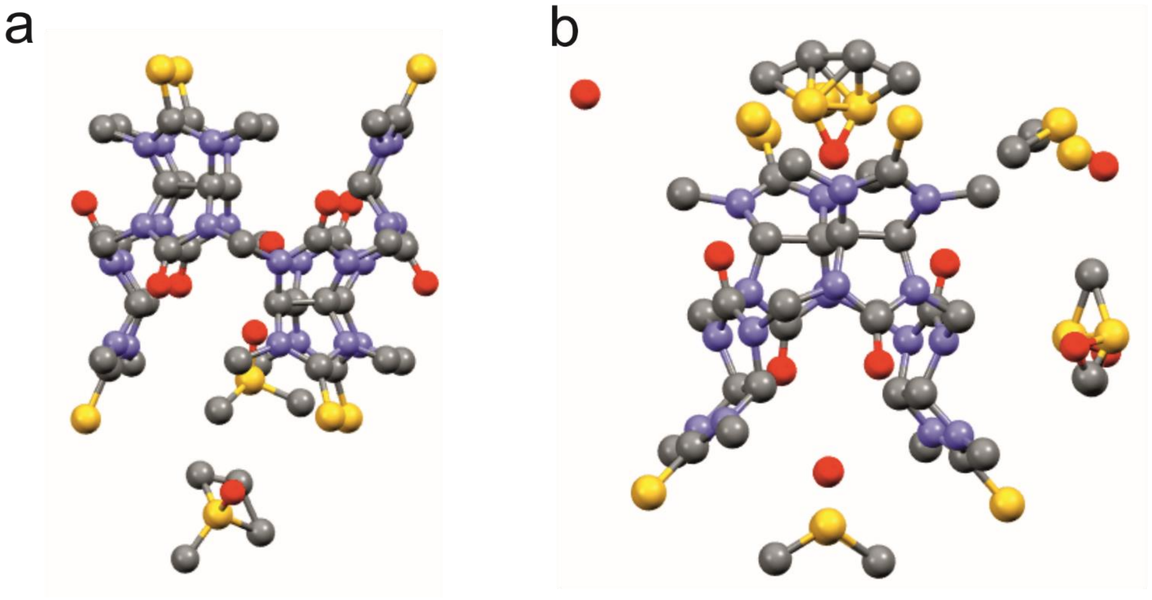

Figure S1. X-ray structures of (a) semithio-BU[4] (**1**) and (b) semithio-BU[6] (**2**) with solvent molecules shown (see main text, ref 29). Hydrogen atoms were omitted for clarity (unit cells with solvent shown in Figure S1). Color code: oxygen, red; sulfur, yellow; nitrogen, blue; carbon, grey.

Table S1. Summary of the SAM contact angles measurement at various temperature conditions.

SAM	Contact angles			
	Bare gold substrate	24 °c	50 °c	80 °c
1	72	52	55	59
2		58	60	63

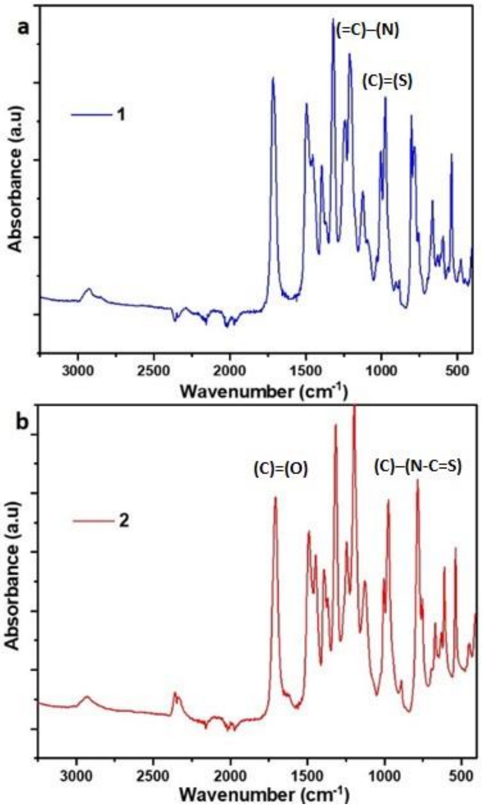

Figure S2. IRRAS spectra of (a) **1** and (b) **2** SAMs on gold prepared by immersion method.

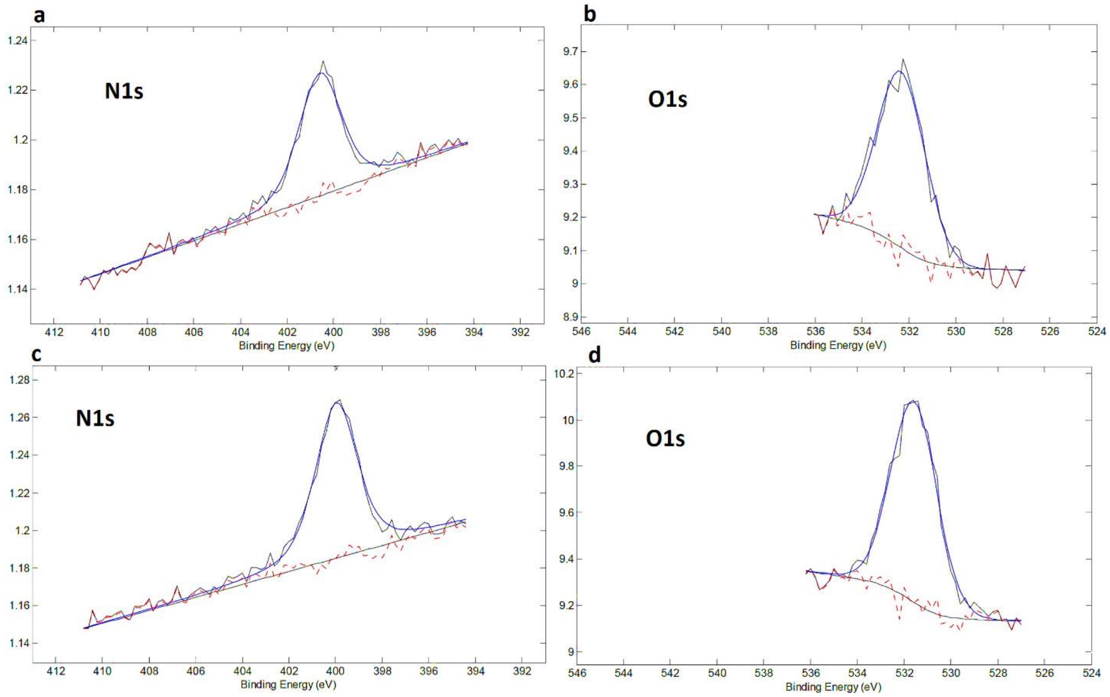

Figure S3. XPS high-resolution N1s and O1s spectra of (a, b) **1** and (c, d) **2** SAMs on gold (same samples as for Figure 2 in the main text).

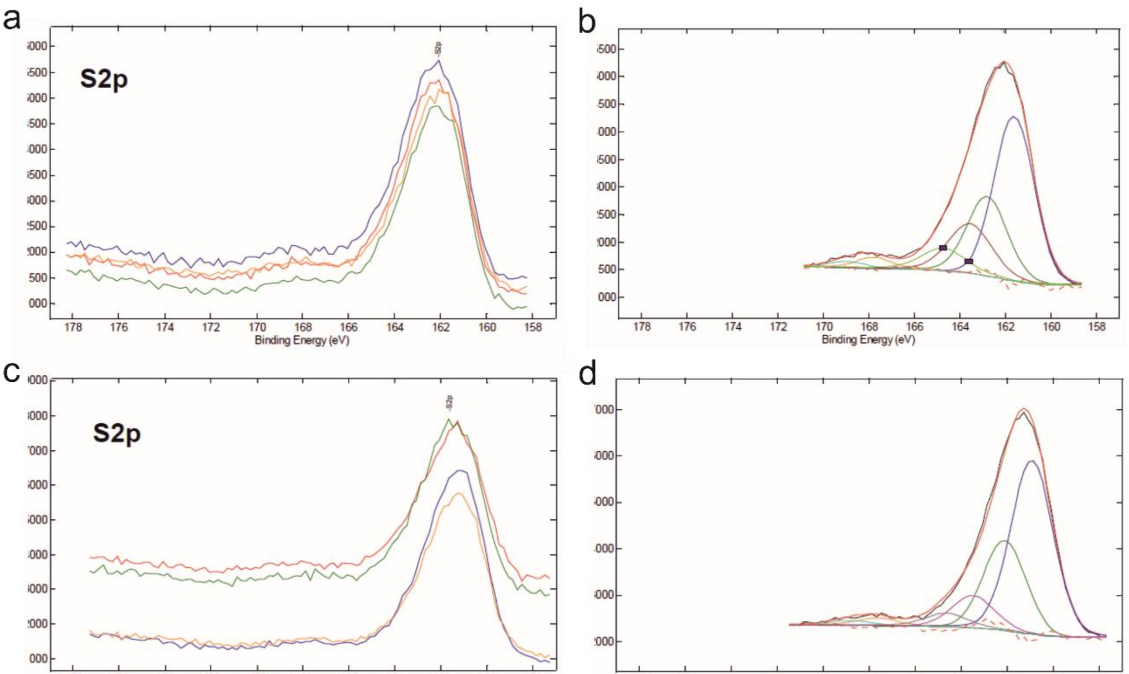

Figure S4. XPS high-resolution of S2p spectra of (a/b) **1** and (c/d) **2** powder samples on indium foil substrate: a/c: Four points per sample were measured during element spectra measurements; b/d: averaged signals with fits with three doublets (two for the main peak, and one for the oxidized signal).

Table S2. Overview table of atomic % and ratios of elements by XPS elemental scans of **1** and **2**, in both SAM (prepared at 80 °C) and powder forms (1 sample each, values are averages for 4 spots per sample).

Sample	%C	%N	%O	%S	N/C	S/C	S/N
1 SAM	57.9	17.0	11.4	13.7	0.29	0.24	0.81
2 SAM	58.0	22.1	14.1	5.9	0.38	0.10	0.27
1 powder	61.1	21.6	12.5	4.9	0.35	0.08	0.23
2 powder	56.6	29.1	9.9	4.5	0.51	0.08	0.15
Calculated	44.7	29.8	8.5	17.0	0.67	0.38	0.57

The experimental values are without taking the %Au values (approx. 50% in the SAM spectra, 0% in the powder spectra) into consideration, and the calculated values are without H.

Discussion of the XPS results

Generally, all SAM spectra were rather noisy, because of the thin molecular architecture (also witnessed by the Au signal that is always visible for approx. 50% in the SAM samples). The S signals are especially noisy because of the low intrinsic sensitivity of S (also indicated by the fact that all measured %S values are lower than the theoretically predicted one; see Table S2). These aspects makes proper quantitative analysis difficult. Yet, SAM samples were made at both 25 and 80 °C, and their XPS spectra were qualitatively highly comparable. Also, SAMs made using **1** and **2** with an associated salt (tetraphenyl phosphonium bromide; data not shown) yielded comparable spectra, indicating no signs of Br or P which indicates that the salt was removed during the SAM preparation.

Regarding the positioning of the S signals, it has been noted in the main text that the S signal of the SAM samples is indicative of mostly unoxidized, Au-bound sulfur, with a small fraction of oxidized sulfur. The latter is also visible in the powder spectra (Figure S4). Most striking is that the position of the main S peak in the powder spectra does not clearly match with unbound sulfur, and the peak is also broader than would agree with a single form of S. At the moment, we do not have a conclusive answer to this. The tested samples are so-called salt-free compounds, i.e. without an anion in the cavity (and the loosely associated cation that goes with it). Instead, the cavity is filled with solvent (DMSO resulting from the synthesis procedure), which is also visible in the crystal structures reported earlier (see Figure S1). Obviously DMSO will affect the elemental composition of the powder spectra, whereas it will most likely not affect the SAM values because the DMSO is rinsed away during the dissolution and macrocycle adsorption process for the SAM preparation. Potentially, the smaller doublet in the main peak of the powder spectra, found at 163.5 eV (26% and 16% of the main peak area for **1** and **2**, respectively) corresponds to the unbound, native bambusurils. Yet, assigning the main doublet at 161.6 or 160.9 eV to DMSO is highly unlikely, because its oxidized nature would put it at higher eV values. We conclude that, because of the intrinsic cleaning procedure of the compound during SAM formation, resulting in the apparent cleaner and narrower S signal and understandable position, the SAM results indicate good-quality SAMs with all/most sulfur attached to gold (result presented in the main text), while the powders would need further study (e.g. by regular elemental analysis).

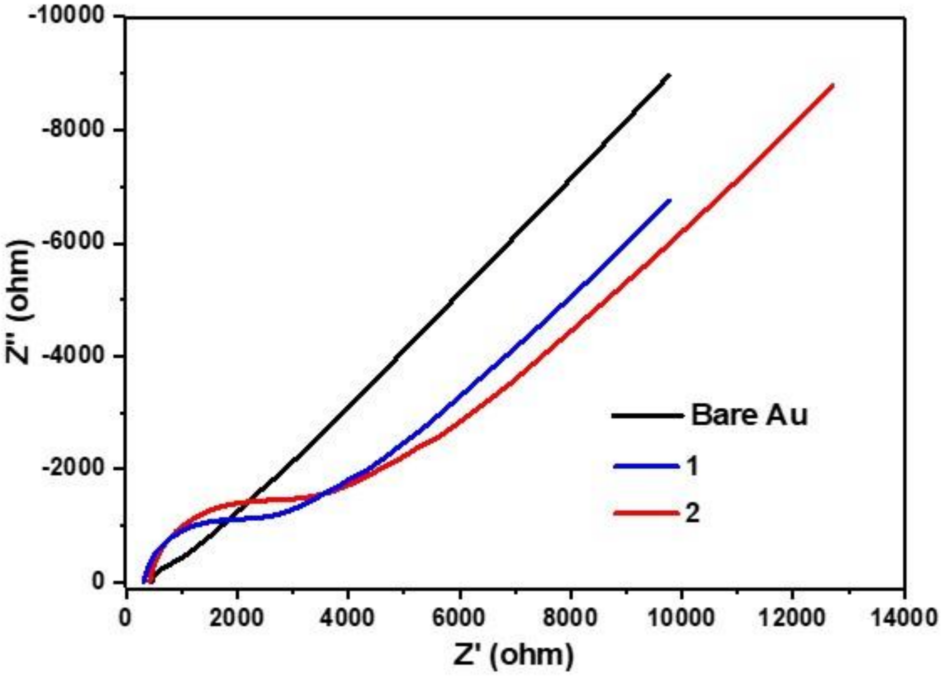

Figure S5. Nyquist plots showing electrochemical impedance spectroscopy responses for bare Au (black), **1** (blue) and **2** (red) SAMs.

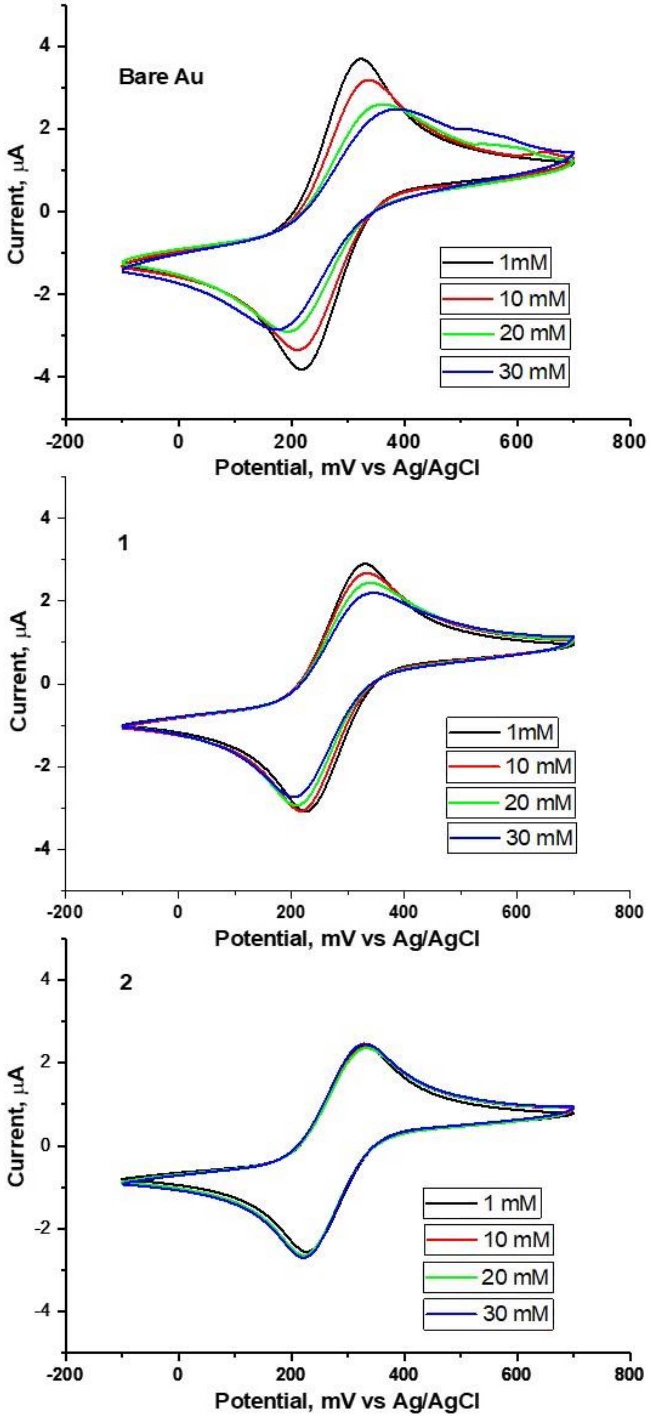

Figure S6. Cyclic voltammogram (CV) of bare Au, **1** and **2** SAM covered gold electrodes. Supporting electrolyte was in 0.5 M K_2SO_4 + 2 mM $Fe(CN)_6^{3-/4-}$ redox species with various concentration of KBr (1 mM to 30 mM), scan rate 100 mV/sec.

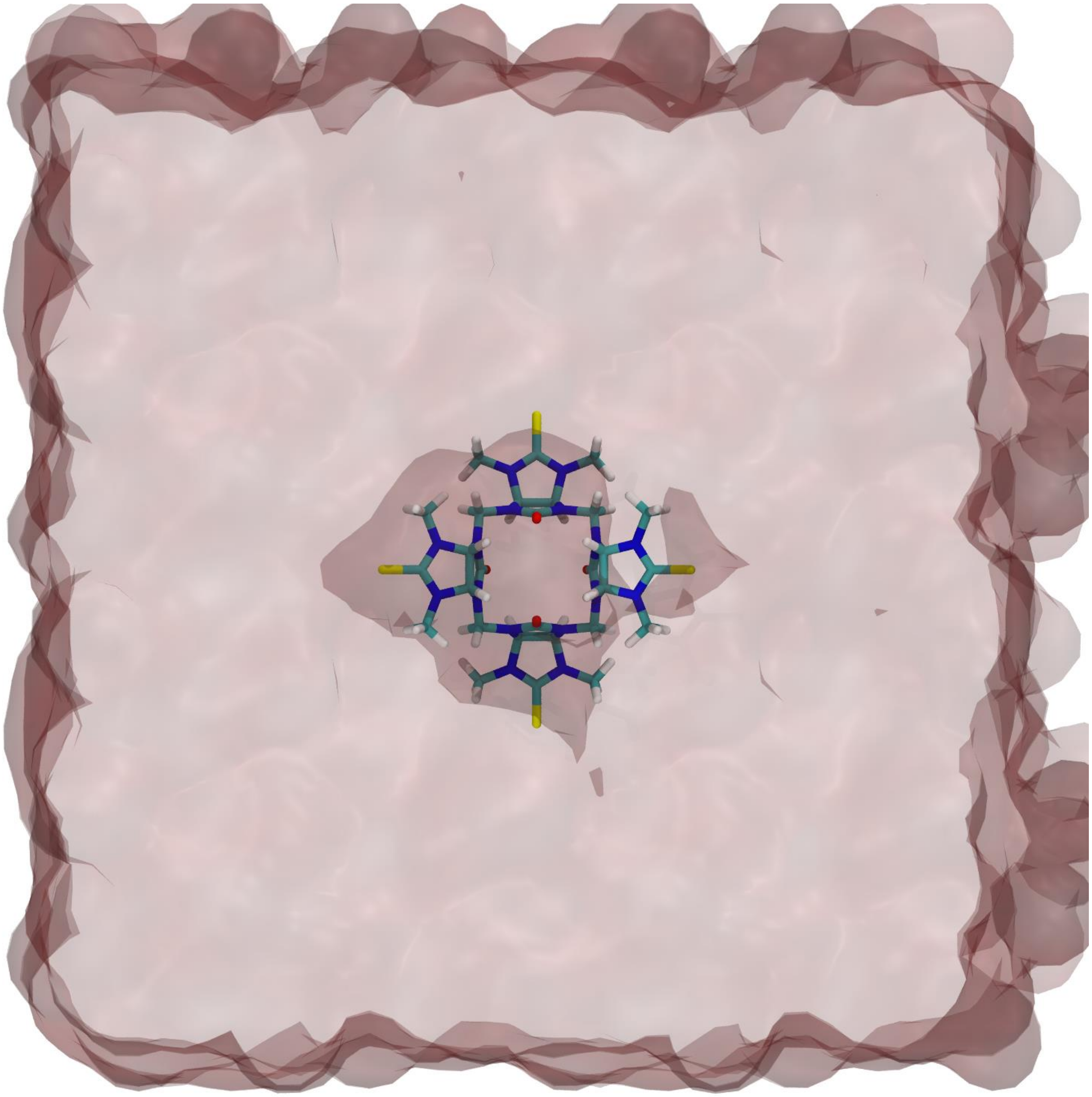

Figure S7. Initial structure of *semithio*-BU[4], **1** MD simulation in water. The *semithio*-BU[4], **1** is depicted with a stick model. The water is depicted as a transparent red volume.

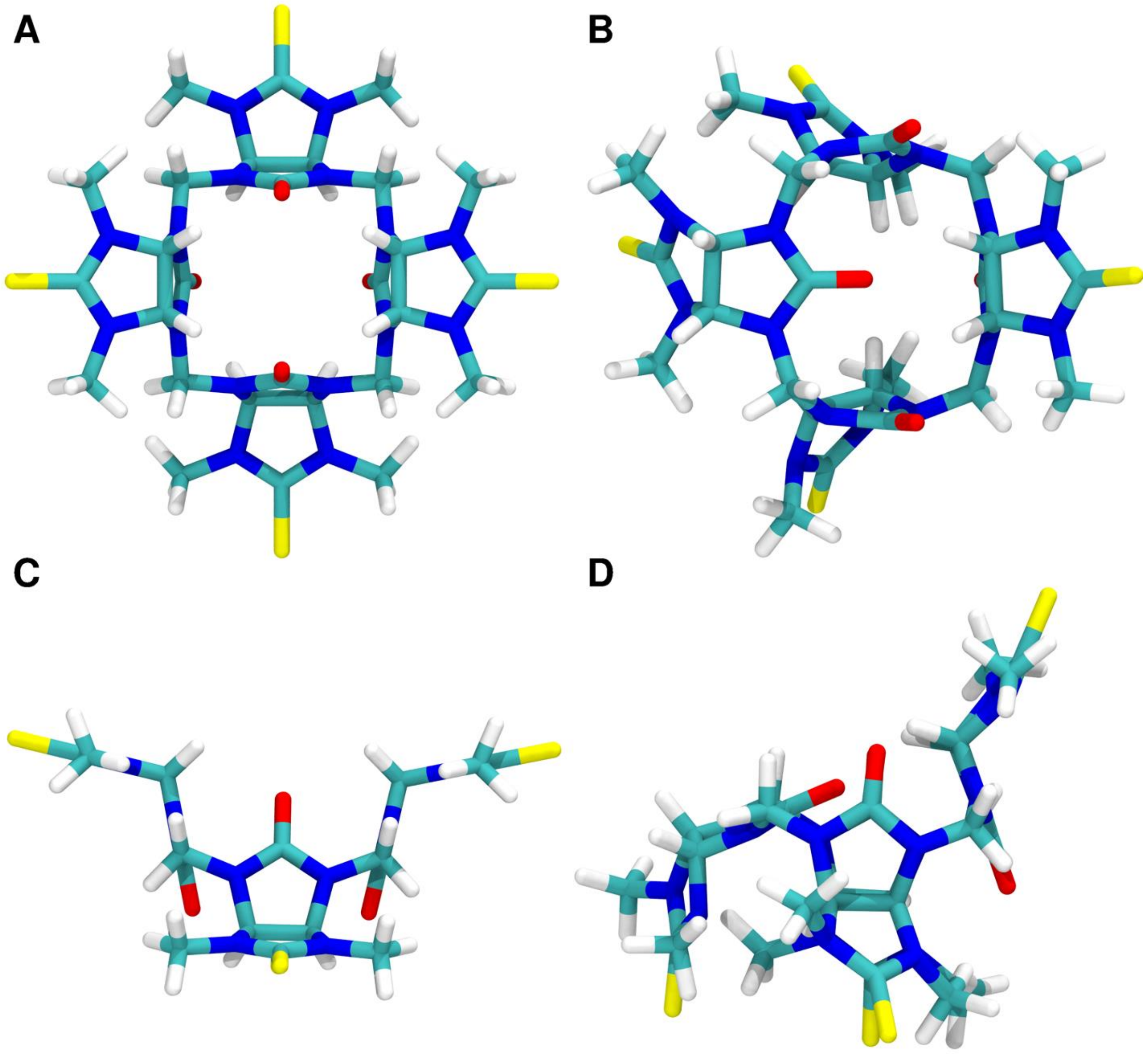

Figure S8. Initial (A/C) and final (B/D) structures of *semithio*-BU[4], **1** MD simulation in water without gold surface. Top panels are projected in the *(x, y)* plane. The bottom panels are projected the *(x, z)* plane. Molecules are depicted with a stick model.